Molecular Communication with Finite-Length Transmitter in Time Dependent Diffusive Channel

Neha Bhusari
Department of Electronics and Communication Engineering
Visvesvaraya National Institute of Technology
Nagpur, India
neha.bhusari10@gmail.com

Avinash G. Keskar
Department of Electronics and Communication Engineering
Visvesvaraya National Institute of Technology
Nagpur, India
agkeskar@ece.vnit.ac.in

Nikhil Sharma
Department of Electronics and Telecommunication Engineering
Military College of Telecommunication Engineering
Mhow, India
nikhilsharma.nit90@gmail.com

Prabhat Kumar Sharma
Department of Electronics and Communication Engineering
Visvesvaraya National Institute of Technology
Nagpur, India
prabhatmadhavec1@gmail.com

***Abstract*—This paper presents a one-dimensional (1-D) molecular communication (MC) model with a finite-length transmitter (TX) under anomalous diffusion characterized by time-dependent diffusivity capturing sub- and super-diffusive behaviors. The receiver (RX) is modeled as a fully absorbing entity placed at a fixed distance. The analytical expressions are derived for the concentration function, the first hitting time density (FHTD), the pulse peak times and channel impulse response (CIR). A peak-time based synchronization scheme is proposed for estimating unknown transmission times. System performance is evaluated in terms of error probability and receiver operating characteristics (ROC) under inter-symbol interference (ISI) and multiple source interference (MSI). Monte Carlo simulations validate the analytical results, revealing the impact of diffusion coefficient, slot duration, and TX length on detection performance.**

***Index Terms*—Molecular communication, finite-length transmitter, time-dependent diffusivity, transmission time estimation, channel impulse response.**

I. Introduction

MOLECULAR communication (MC) is a significant emerging field that replicates nature-inspired chemical signaling to enable communication in non-electromagnetic environments [1]. Bio-compatible artificial nanomachines can actively participate in MC, functioning as transmitters (TX), receivers (RX), or supervisory nodes [2]. With this, MC has potential for a wide range of biomedical applications, including early disease detection, anomaly monitoring, and targeted drug delivery [3]. In the *in vivo* environment, there are multiple possibilities for both intra-cellular and extra-cellular communication through diffusion [4]. The dynamics of biological entities, such as cells, often depend on physiological characteristics like shape, size, and diffusivity [5]. Consequently, various dimensional models, including one-dimensional (1-D) and three-dimensional (3-D), have been studied for communication within bounded [6], unbounded [7], spherical [8], and cylindrical [9] media. This way different TX and RX architectures, defined by their geometry and molecule release methods, are examined [3]. In the nanoscale environment, molecular transport often exhibits anomalous diffusion where the mean square displacement of molecules scales non-linearly with time as $< x^2(t) > \propto t^\beta$ than classical diffusion phenomenon. It is due to heterogeneous medium properties, crowding effects, and temporal correlation in particle motion [10]. Time dependent anomalous diffusion models effectively capture these dynamics by accounting for memory effects. This leads to more realistic channel characterization and improved performance.

However, most models consider point TXs, whereas in practical scenarios, TXs can have a finite spatial extent. This geometric difference alters the molecular propagation dynamics. Most existing works assume synchronized TX and RX [10] which is practically challenging due to independent clocks. To the best of our knowledge, limited work has explored time dependent anomalous diffusion channels with non-point elongated finite-length TXs[1] in the context of time synchronization. Specifically, following are the main contributions of this work:

1) The time dependent diffusivity is considered in a 1-D channel with finite length TX. The Greens concentration function solution and first hitting time density (FHTD) are derived with absorbing RX.
2) The pulse peak time expressions corresponding to the concentration function and FHTD are derived.
3) A peak-time estimator is proposed for time synchronization, enabling estimation of unknown transmission time.
4) The performance of channel is evaluated in terms of probability of error ($\overline{P}_e$) and receiver operating charac-

This work is supported by the core research grant (CRG/2023/009061) of Anusandhan National Research Foundation (earlier Science and Engineering Research Board), Government of India.

[1]The considered finite-length TX and 1-D anomalous diffusion channel are motivated by elongated biological structures such as mitochondria and endothelial cells [5], where transport often exhibits anomalous diffusion due to cellular crowding.

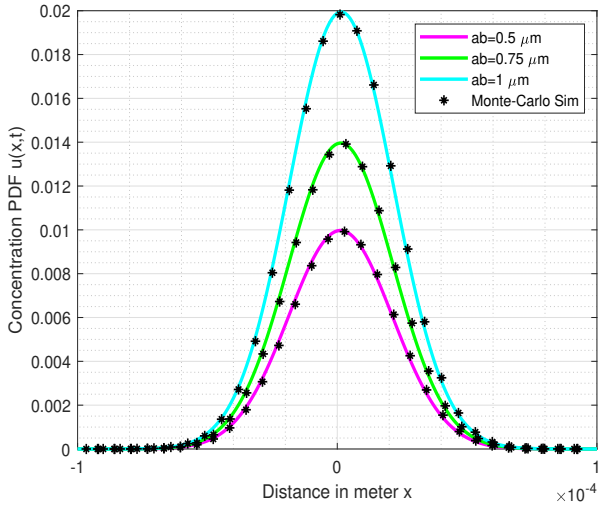

Fig. 1. Concentration function with finite-length TX for unbounded channel when x_a = 1μm and x_b are 1.5μm, 1.75μm and 2μm

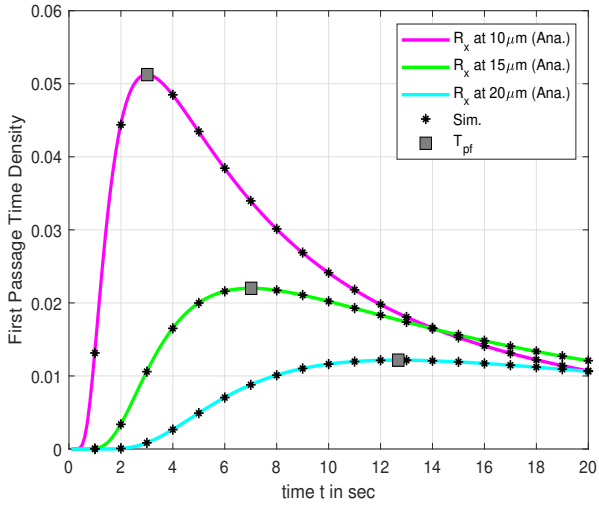

Fig. 2. First passage time density for molecule release for bounded channel when TX is of length 1μm and RX at 10μm,15μm and 20μm

teristics (ROC) under ISI and MSI, validated via Monte Carlo simulations, with insights into the impact of TX length, slot duration, and diffusion coefficient.

The rest of this paper is organized as follows: System model is described in Section II. Section III conducts the mathematical analysis with respect to channel impulse response (CIR) of the proposed system. Section IV describes the communication channel. We have verified our analysis with numerical results and simulations in Section V, and concluded in Section VI.

II. Time Dependent Diffusive System Model

We consider a time dependent diffusive MC system where a finite-length TX of length $x_a x_b$ releases molecules at time t_0. A fully absorbing RX is placed at a distance x_c from the TX center. Using ASK modulation, the TX releases M molecules with probability ρ for bit-1 and none for bit-0. The molecules propagate through Brownian motion according to Fick's diffusion law. Both TX and RX are assumed to be working at uniform viscosity and temperature. The information theoretic modeling is used for analyzing the end-to-end system performance. Let $u(x,t)$ be the molecules concentration at position x and time t. The initial condition assigns $u(x_a, x_b, t_0) = M$ for $x_a < x < x_b$, and zero outside this interval, where M denotes the uniform initial concentration density across the TX.

A. Concentration Function with Time Dependent Diffusivity

Anomalous diffusion in an infinite unbounded 1-D $(-\infty < x < \infty)$ medium is modeled by a fractional diffusion equation [10] given by $\frac{\partial u(x,t)}{\partial t} = \beta t^{\beta-1} D \frac{\partial^2 u(x,t)}{\partial x^2}$, where $\beta \in [0,2]$ is the anomalous diffusion exponent. It characterizes normal diffusion ($\beta = 1$), sub-diffusion ($\beta < 1$), and super-diffusion ($\beta > 1$) [11]. The solution to this diffusion equation is derived as

$$u(x,t) = \frac{M}{2}\left[\text{erf}\left(\frac{x_b - x}{\sqrt{4Dt^{\beta}}}\right) - \text{erf}\left(\frac{x_a - x}{\sqrt{4Dt^{\beta}}}\right)\right] \quad (1)$$

Fig. 1 plots (1), concentration function versus distance at 2 seconds. With $x_a = 1\mu$m fixed and varying x_b, the analytical results match Monte Carlo simulations with 10^4 runs. Increasing TX length enhances propagation range and leads to increase in molecule concentration at the RX.

B. First-hitting Time Density

The FHTD is the first arrival probability at x_c at time t, with an absorbing RX at x_c resulting in a semi-infinite channel $(-\infty < x < x_c)$.

Lemma 1: The FHTD of molecules arrival is derived as

$$f_p(t) = M\beta\sqrt{\frac{Dt^{\beta-2}}{\pi}}\left[e^{-\frac{(x_c-x_b)^2}{4Dt^{\beta}}} - e^{-\frac{(x_c-x_a)^2}{4Dt^{\beta}}}\right] \quad (2)$$

Proof: The proof of (2) is given in Appendix.

Fig. 2 shows the FHTD function derived in (2) which is verified with Monte Carlo simulations. It is seen that the peak time is delayed as TX-RX distance increases.

Lemma 2: The pulse peak time with respect to concentration function and FHTD are obtained as shown in (3) and (4).

Proof: The pulse peak time [8] can be obtained by differentiating (1) with time and obtaining the maxima of the equation. The pulse peak time expression at x is obtained as

$$T_{pu} = \left[\frac{(x_b + x_a - 2x)(x_b - x_a)}{4Dln(\frac{x_b - x}{x_a - x})}\right]^{\frac{1}{\beta}} \quad (3)$$

Note that for normal diffusion and a point TX the pulse peak time reduces to $T_{pu} = \frac{(x-x_a)^2}{2D}$ which is same as given in [10]. The peak time of FHTD is derived using the same approach for (2) as of T_{pu}, resulting in T_{pf}.

$$T_{pf} = \left[\frac{\beta^2[(x_c - x_a)^2 + (x_c - x_b)^2]}{4D(4 - \beta^2)}\right]^{\frac{1}{\beta}} \quad (4)$$

For normal diffusion and negligible TX size ($x_c \gg x_a x_b$), this reduces to an ideal value of $T_{pf} = \frac{(x_c - x_a)^2}{6D}$ [10]. In Fig. 2,

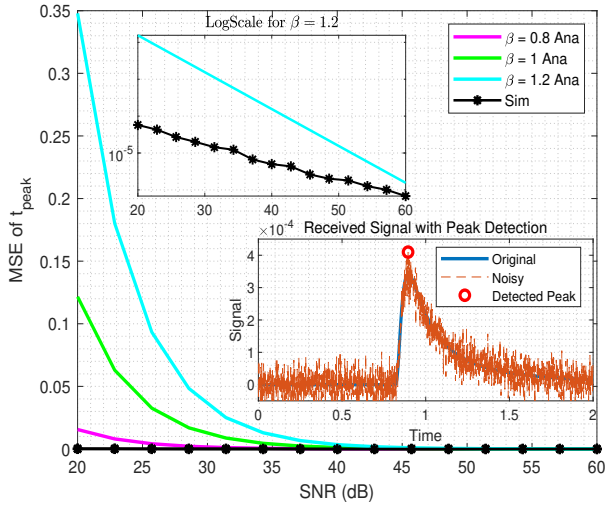

Fig. 3. MSE of peak-time estimation versus SNR for different β values. The inset shows the log-scale view for $\beta = 1.2$ and the received signal with detected peak.

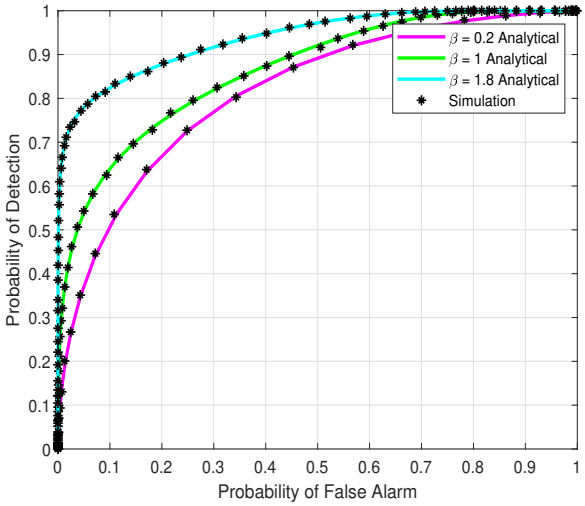

Fig. 4. ROC with sub-diffusive, normal and super-diffusive channel when RX is at 10 μm

the observed peak times match the analytical values from (4). The values are 3, 7, and 12.7 s which are indicated by square markers aligning with simulations.

C. Channel Impulse Response

The CIR is defined by $C_p(\hat{T}) = \int_0^{\hat{T}} f_p(t), dt$. Thus, the same probability of molecules arriving at the RX within time $\hat{T}$ is derived as

$$C_p(\hat{T}) = \frac{M}{2\sqrt{\pi}} \left[(x_c - x_b)\Gamma\left(-\frac{1}{2}, \frac{(x_c - x_b)^2}{4D\hat{T}^\beta}\right) - (x_c - x_a)\Gamma\left(-\frac{1}{2}, \frac{(x_c - x_a)^2}{4D\hat{T}^\beta}\right)\right] \quad (5)$$

III. Transmission Time Estimation

The proposed time synchronization framework implement peak time based estimator which utilizes the temporal characteristics of the received signal u_r. When molecules are emitted at an unknown transmission time T_{tx} under anomalous diffusion, the RX estimates the propagation delay as $\hat{\tau} = t_{\text{peak}}$ as defined in (3). The observed peak timestamp at RX affected by the clock offset is $T_{rx}^{\text{peak}} = \arg\max(u_r)$. The transmission time is then estimated as $\hat{T}_{tx} = T_{rx}^{\text{peak}} - \hat{\tau} - \phi$, where $\hat{\tau}$ represents the delay inferred from the received signal profile and is independent of clock mismatch, and ϕ denotes the clock offset[2] which can be estimated similarly. In case of reactions, it affects scale amplitude without altering delay. This preserves the simplicity and robustness of the peak-based estimator.

At SNR = 20 dB, with $T_{tx} = 0.5$ s, $\hat{\tau} = 0.1$ s after T_{tx}, and $\phi = 0.3$ s, the peak is observed at $T_{rx}^{\text{peak}} \approx 0.89$ s. This yield almost zero MSE and hence, accurate recovery of Ttx. The offset is estimated as $\hat{\phi} = T_{rx}^{\text{peak}} - T_{tx} - \hat{\tau} = 0.3032$ s with MSE 1.915×10^{-4}. Thus, after T_{rx}^{peak}, the true $t_{\text{peak}} = 9.5 \times 10^{-2}$ s and estimated 9.8×10^{-2} s with MSE 1.92×10^{-4}. Fig. 3 exhibits that the MSE of t_{peak} decreases as SNR increase $\forall\beta$. This indicates improved estimation accuracy with high signal quality. Lower β gives smaller error due to sharper peaks, while for higher β, MSE increases due to broad concentration profiles (3). The close agreement between analytical and simulation results further validates the theoretical model. Overall, the approach of peak timing estimation achieves accurate synchronization under moderate noise by separating delay from clock offset and it is is strongly governed by the diffusion dynamics characterized by β.

[2]The received concentration profile is used to estimate the propagation delay $\hat{\tau}$ through the peak location. The clock offset ϕ is then obtained using sequence with known transmission instants, which gives $\hat{\phi} = T_{rx}^{\text{peak}} - T_{tx} - \hat{\tau}$.

IV. Communication Channel Model

The communication channel model in the proposed 1-D timely anomalous diffusive MC system is divided into N time slots with duration τ where n^{th} time slot period can be given as $[(n-1)\tau, n\tau]$ and $n \in \{1, 2, ...N\}$. The bit sequence to be transmitted and received in N slots is represented by T_N and R_N whereas bit transmitted and received in n^{th} time slot is denoted by $t[n]$ and $r[n]$ respectively such that $T_N = t[1], t[2], t[3], ..., t[N]$ and $R_N = r[1], r[2], r[3], ..., r[N]$. Let the arrival probability that a molecule reaches RX in n^{th} time slot when transmitted in m^{th} time slot is denoted by p_{n-m} and p_0 be the probability that a molecule received within the same time slot of transmission i.e. $m = n$. Thus the arrival probability p_{n-m} is given by $p_{n-m} = C_p((n-m+1)\tau) - C_p((n-m)\tau)$ where $C_p(t)$ is as given in (5).

A. Received Information Characteristics

The communication performance of the system is analyzed in this section. Let $R[n]$ be the total number of received molecules in the n^{th} time slot where received signal is a combination of molecules which are received in the desired time slot and interfering time slots. MSI is also taken into

account. Hence $R[n]$ is expressed as $R[n] = R_C[n] + R_I[n] + R_M[n]$ where $R_C[n]$ are the molecules received in current time slot following Binomial distribution i.e. $R_C[n] \sim Binomial(Mt[n], p_0)$, where $t[n] \in \{0, 1\}$ is the information symbol transmitted in n^{th} time slot. The term $R_I[n]$ denotes molecules received from all previous time slots than n^{th} time slot i.e. ISI such that $R_I[m] \sim Binomial(Mt[n-m], p_{n-m})$ where p_{n-m} is arrival probability of the previous m^{th} time slot. The final term denotes MSI following the Poisson distribution such that $R_M[n] \sim Poisson(\lambda_M[n])$ [12]. It is observed that the Poisson approximation is more relevant for the binomial distribution, while a Gaussian approximation can show noticeable loss in precision [13], [14]. Hence, by approximating the terms $R_C[n]$ and $R_I[n]$ with average rates $\lambda_C[n]$ and $\lambda_I[n]$ respectively such that $R_C[n] \sim Poisson(Mt[n]p_0)$ and $R_I[n] \sim Poisson(M \sum_{m=1}^{n-1} t[n-m]p_{n-m})$.

B. Detection Performance Analysis

The information symbol detection problem at RX can be defined in terms of null hypothesis H_0 and alternative hypothesis H_1 with respect to the transmission of binary symbols and it is given by $H_0 : R[n] = R_I[n] + R_M[n]$ and $H_1 : R[n] = R_C[n] + R_I[n] + R_M[n]$. The number of molecules $R[n]$ received at the RX corresponding to this binary hypotheses are $Poisson$ distributed with parameters $\lambda_0[n]$ and $\lambda_1[n]$ respectively, where $\lambda_0[n] = \lambda_I[n] + \lambda_M[n]$ and $\lambda_1[n] = \lambda_C[n] + \lambda_I[n] + \lambda_M[n]$. To find optimum threshold at RX, log likelihood ratio test is used and given by $ln\left[\frac{Pr(R[n]|H_1)}{Pr(R[n]|H_0)}\right] \underset{H_0}{\overset{H_1}{\lessgtr}} ln\left[\frac{1-\rho}{\rho}\right]$ where the probabilities are defined as $Pr(R[n]|H_1) = \sum_{k=1}^{Th[n]} \frac{e^{-\lambda_1[n]}(\lambda_1[n])^k}{k!}$ and $Pr(R[n]|H_0) = \sum_{k=1}^{Th[n]} \frac{e^{-\lambda_0[n]}(\lambda_0[n])^k}{k!}$ such that $Th[n]$ is the optimal decision threshold depending on which the decision rule is defined as $r[n] = 1$ if $R[n] \geq Th[n]$ and 0 otherwise. The expression for optimal threshold Th[n] [15] is given by $Th[n] = \frac{ln(\frac{1-\rho}{\rho}) + Mp_0}{ln(\lambda_1[n]) - ln(\lambda_0[n])}$.

C. Probability of Detection and False Alarm

The probability of error expression for n^{th} time slot is defined as $P_e[n] = (1-P_D[n])\rho + P_{FA}[n](1-\rho)$ where $P_D[n]$ i.e. detection probability and $P_{FA}[n]$ false alarm probability can be given as $P_D[n|{T_N}^{n-1}] = 1 - Pr(R[n]|H_1)$ and $P_{FA}[n|{T_N}^{n-1}] = 1 - Pr(R[n]|H_0)$ [9]. Hence, the average probability of error is $\overline{P}_e = \frac{1}{N} \sum_{n=1}^{N} P_e[n]$.

V. Numerical Analysis

In this section, numerical analysis of the given anomalous diffusive channel is presented in terms of $\overline{P}_e$ and ROC with Monte-Carlo simulations for 10^4 samples. Simulations are conducted for 5 time slots with 100 molecules releasing for bit '1'. The transmitted symbols are considered to be equiprobable and rate constant for MSI is 10.

Fig. 4 shows the ROC for different β with TX length 1 μm and RX at 10 μm. For a fixed false alarm rate, super-diffusive channels achieve higher detection probability, This yields the largest ROC area due to higher effective diffusion. Fig. 5 shows that increasing slot duration τ from 1 s to 3 s improves ROC performance, yielding higher detection probability due to increased symbol separation. Fig. 6 shows $\overline{P}_e$ for TX lengths 0.5–1 μm. For low error values (< 0.1), the optimal threshold increases with TX length due to the larger spatial distribution of molecules. The shorter TX leads to a higher error. Fig. 7 shows $\overline{P}_e$ versus threshold for $D = 50$–$200\mu m^2$/s. Increasing D reduces error from ≈ 0.41 to ≈ 0.035 due to increased mean square displacement of molecules.

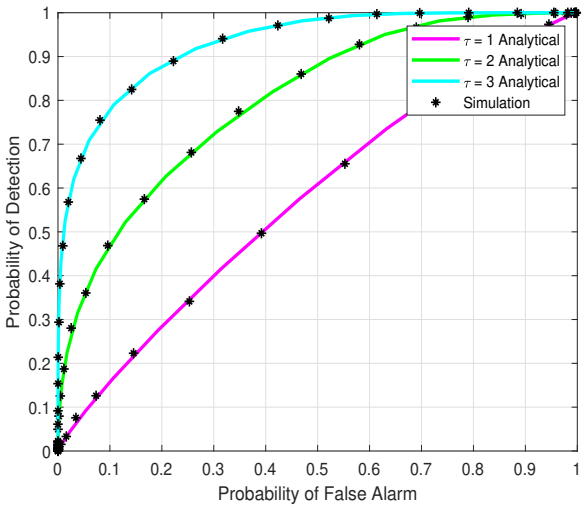

Fig. 5. ROC with varying slot duration of 1 s, 2 s and 3 s when RX is at 50 μm

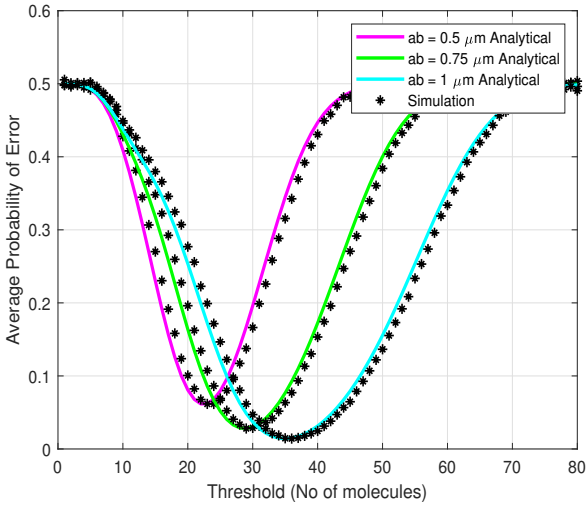

Fig. 6. Probability of error with varying length of TX as $x_a x_b$ = 0.5 μm, 0.75 μm and 1 μm

VI. Conclusion

This paper develops a 1-D anomalous diffusion based MC framework with a finite-length TX and an absorbing RX. Closed form expressions for the concentration, FHTD, CIR, and peak times are derived, along with a peak-based

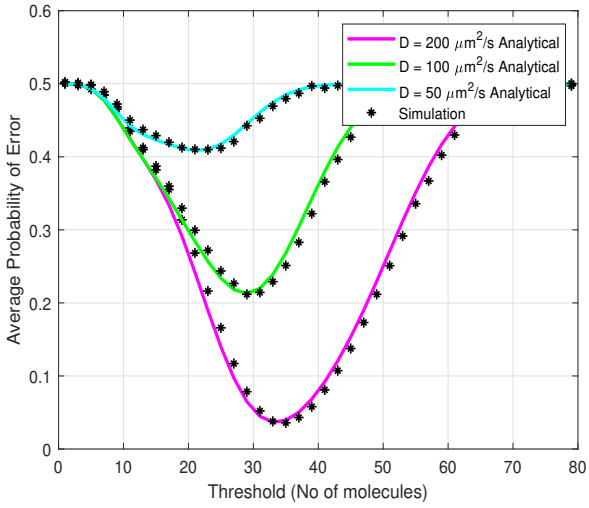

Fig. 7. Probability of error with varying diffusion coefficient as 200 $\mu m^2/s$, 100 $\mu m^2/s$ and 50 $\mu m^2/s$ for RX at 30 μm

estimator enabling time synchronization and transmission time detection. Performance analysis shows that higher diffusion constant, super-diffusion i.e. higher mean square displacement of molecules and well seperated symbols with larger time slot duration improves detection, while reduced TX length increases error. Monte Carlo results closely validate the analytical expressions. Future work includes extending the model to reactive 3-D environments.

Appendix
Proof of First Hitting Time Density

Let x_a and x_b denote the finite-length TX boundaries and x_c the absorbing boundary satisfying $u(x_c,t)=0$. Using the random walk interpretation of molecular diffusion under the assumption that their movement is independent and in unit steps. With the method of images, the PDF is obtained by superposing the unbounded diffusion PDF with that of a mirror image source, yielding

$$u^*(x,t) = \frac{M_0}{2}\left[\text{erf}\left(\frac{x_b-x}{\sqrt{4Dt^\beta}}\right) - \text{erf}\left(\frac{x_a-x}{\sqrt{4Dt^\beta}}\right) + \text{erf}\left(\frac{2x_c-x_b-x}{\sqrt{4Dt^\beta}}\right) - \text{erf}\left(\frac{2x_c-x_a-x}{\sqrt{4Dt^\beta}}\right)\right]. \quad (6)$$

Here (6) satisfy both initial and boundary conditions leading to the new resultant PDF with absorbing RX present at x_c. The probability of molecules existing just before absorption at x_c is called as survival probability [16] $s_p(t)$ which can be obtained by integrating the resultant PDF with respect to distance over the range of available distance for propagation before absorption and is given by $s_p(t) = \int_{-\infty}^{x_c} u^*(x,t)\,dx$. Solving this, we get

$$s_p(t) = \sqrt{\frac{4Dt^\beta}{\pi}}\left[e^{-\left(\frac{x_c-x_a}{\sqrt{4Dt^\beta}}\right)^2} - e^{-\left(\frac{x_c-x_b}{\sqrt{4Dt^\beta}}\right)^2}\right] + (x_c-x_a)\text{erf}\left(\frac{x_c-x_a}{\sqrt{4Dt^\beta}}\right) - (x_c-x_b)\text{erf}\left(\frac{x_c-x_b}{\sqrt{4Dt^\beta}}\right) \quad (7)$$

The first passage time density indicates the rate of absorption which exhibits exponential decay, and can be obtained by differentiating the survival probability with respect to time as in (2).

References

[1] V. Jamali, A. Ahmadzadeh, W. Wicke, A. Noel, and R. Schober, "Channel modeling for diffusive molecular communication—a tutorial review," *Proceedings of the IEEE*, vol. 107, no. 7, pp. 1256–1301, 2019.

[2] S. Kumar, P. K. Sharma, and M. R. Bhatnagar, "Game-theoretic analysis of fusion rules over molecular reporting channels," *IEEE Transactions on NanoBioscience*, vol. 23, no. 1, pp. 101–108, 2024.

[3] N. Farsad, H. B. Yilmaz, A. Eckford, C.-B. Chae, and W. Guo, "A comprehensive survey of recent advancements in molecular communication," *IEEE Communications Surveys Tutorials*, vol. 18, no. 3, pp. 1887–1919, 2016.

[4] B. Alberts, A. Johnson, J. Lewis, M. Raff, K. Roberts, and P. Walter, *Molecular Biology of the Cell*, 4th ed. New York: Garland Science, 2002. [Online]. Available: https://www.ncbi.nlm.nih.gov/books/NBK21054/

[5] H. Lodish, A. Berk, S. L. Zipursky, P. Matsudaira, D. Baltimore, and J. Darnell, *Molecular Cell Biology*. W. H. Freeman and Co., 2020.

[6] W. Guo, Y. Deng, B. Li, C. Zhao, and A. Nallanathan, "Eavesdropper localization in random walk channels," *IEEE Communications Letters*, vol. 20, no. 9, pp. 1776–1779, 2016.

[7] P. Sharma and L. Chouhan, "Performance analysis of diffusive molecular communication in three dimensional channel," 08 2019.

[8] X. Bao, Y. Zhu, and W. Zhang, "Channel characteristics for molecular communication via diffusion with a spherical boundary," *IEEE Wireless Communications Letters*, vol. 8, no. 3, pp. 957–960, 2019.

[9] S. Dhok, L. Chouhan, A. Noel, and P. K. Sharma, "Cooperative molecular communication in drift-induced diffusive cylindrical channel," *IEEE Transactions on Molecular, Biological, and Multi-Scale Communications*, vol. 8, no. 1, pp. 44–55, 2022.

[10] L. Chouhan, P. K. Sharma, and A. Noel, "Molecular communication in fractional diffusive channel," *IEEE Communications Letters*, vol. 24, no. 10, pp. 2172–2176, 2020.

[11] H. J. Kim, "Anomalous diffusion induced by enhancement of memory," *Phys. Rev. E*, vol. 90, p. 012103, Jul 2014.

[12] M. U. Mahfuz, D. Makrakis, and H. T. Mouftah, "A comprehensive analysis of strength-based optimum signal detection in concentration-encoded molecular communication with spike transmission," *IEEE Transactions on NanoBioscience*, vol. 14, no. 1, pp. 67–83, 2015.

[13] A. Noel, K. C. Cheung, and R. Schober, "Improving receiver performance of diffusive molecular communication with enzymes," *IEEE Transactions on NanoBioscience*, vol. 13, no. 1, pp. 31–43, 2014.

[14] H. B. Yilmaz and C.-B. Chae, "Arrival modelling for molecular communication via diffusion," *Electronics Letters*, vol. 50, pp. 1667–1669, 11 2014.

[15] L. Chouhan, P. K. Sharma, and N. Varshney, "Optimal transmitted molecules and decision threshold for drift-induced diffusive molecular channel with mobile nanomachines," *IEEE Transactions on NanoBioscience*, vol. 18, no. 4, pp. 651–660, 2019.

[16] R. Metzler, G. Oshanin, and S. Redner, *First-Passage Phenomena and Their Applications*, 12 2014.